Supporting Information

Self-Assembly of Human Profilin-1 Detected by CPMG NMR Spectroscopy

Enrico Rennella[1], Ashok Sekhar[1], and Lewis E. Kay[1,2]

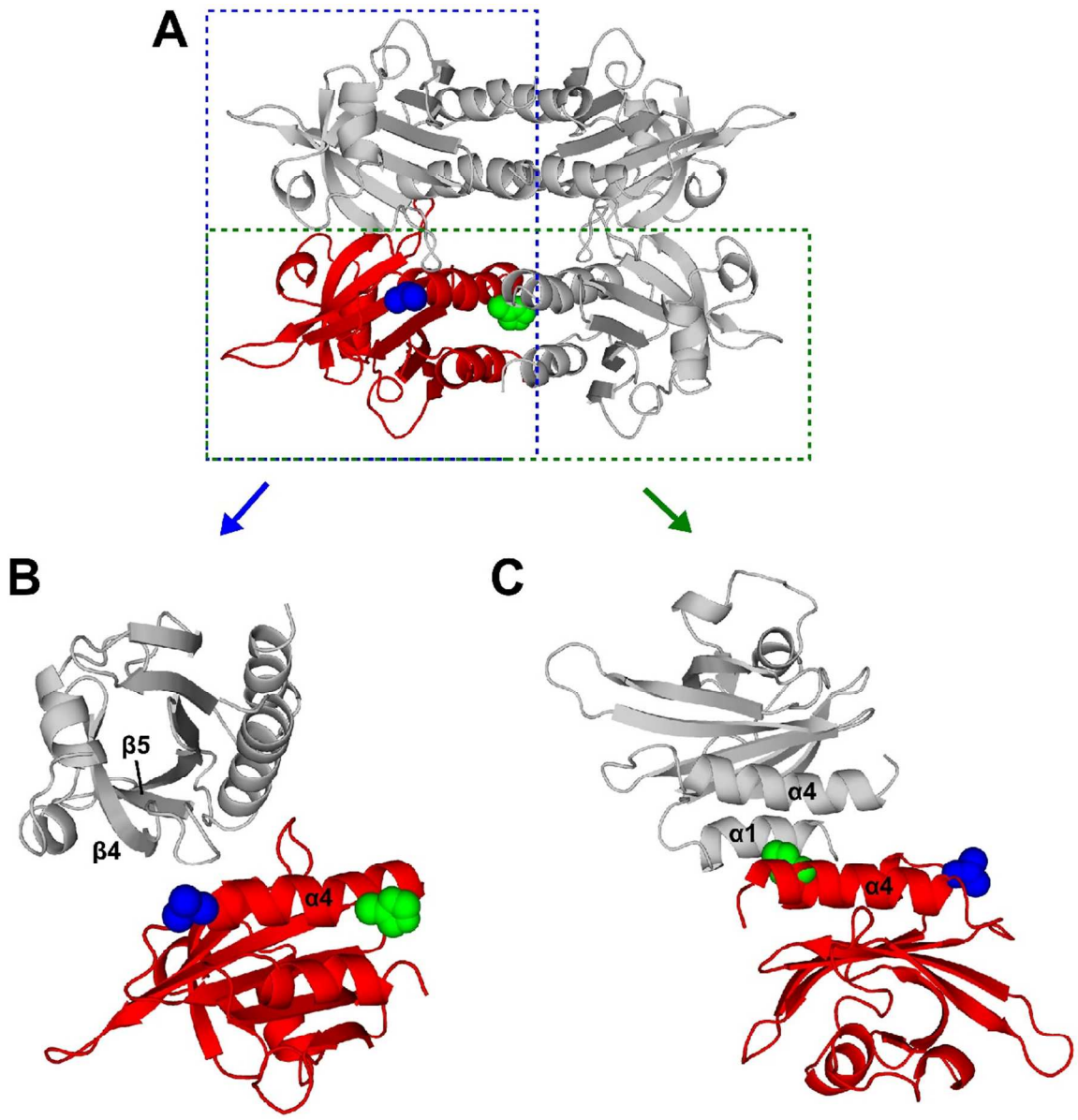

Figure S1. (A) Cartoon of the putative PFN1 tetramer based on the tetrameric X-ray model of PFN2 (PDB ID: 1D1J[1]). Each of the four copies of PFN2 was replaced with the NMR derived structure of monomeric PFN1 (PDB ID 1PFL[2]), using the first of twenty published solution structures. (B-C) Enlarged views of the dimer interfaces stabilizing the tetramer, highlighting Leu^{123} (blue spheres) and His^{134} (green spheres) that are mutated to destabilize the tetramer in solution (see text). The dimer in panel B (blue dashed rectangle in A) is stabilized by the loop between β4-β5 and the N-terminus of α4

including Leu^{123}. The dimer interface in panel C (green dashed rectangle in panel A) comprises α1 of one monomer and the C-terminus of α4 of a second monomer, including His^{134}. Thus the L123R and H134R mutations would be expected to destabilize the interfaces of molecules in panels B and C, respectively.

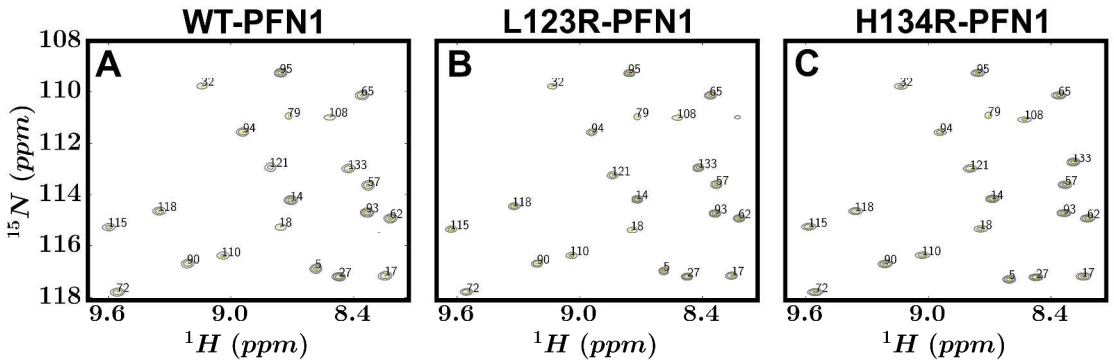

Figure S2. Selected regions of ^{1}H,^{15}N-HSQC spectra of WT, L123R and H134R human PFN1, 10 ^{o}C, 600 MHz.

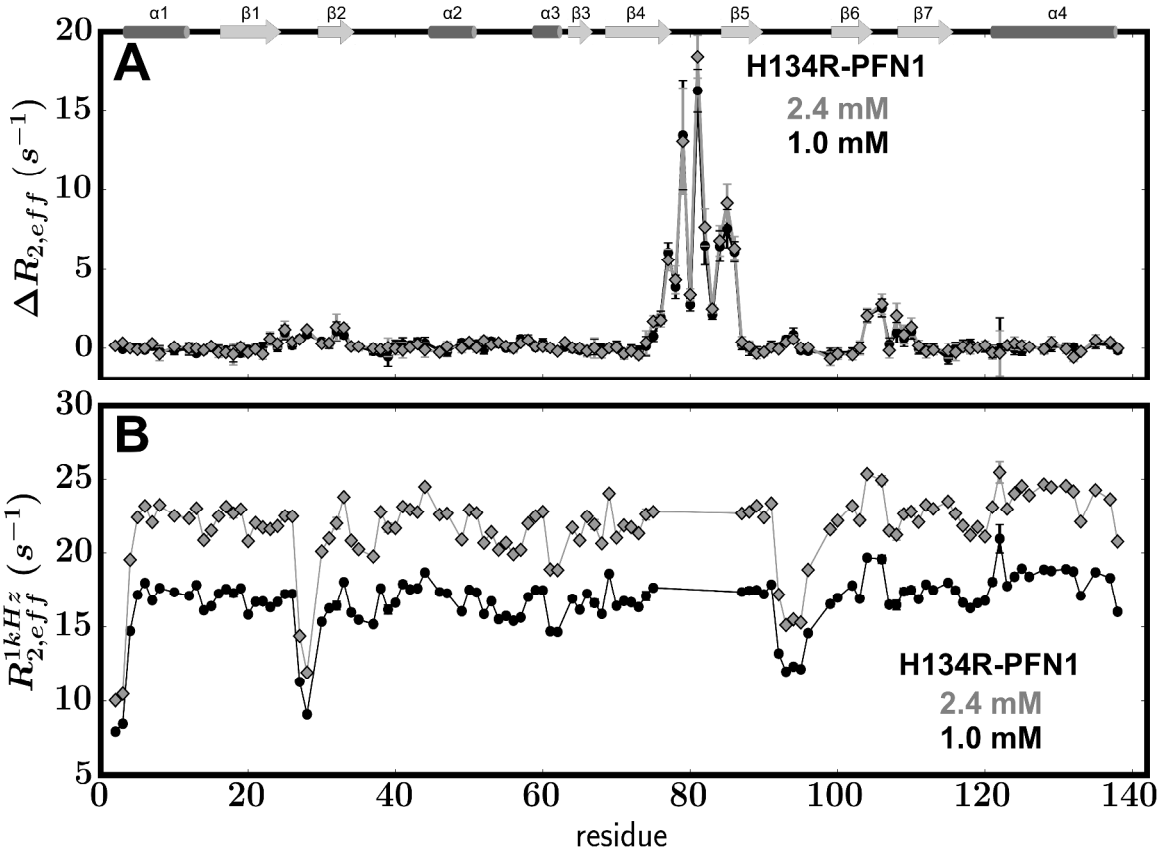

Figure S3. Analysis of in-phase ^{15}N CPMG data acquired on a sample of ^{15}N H134R PFN1 at several protein concentrations, 10°C. $\Delta R_{2,eff} = R_{2,eff}^{30\,Hz} - R_{2,eff}^{1kHz}$ and $R_{2,eff}^{1kHz}$ are plotted for two different concentrations in panels A and B, respectively.

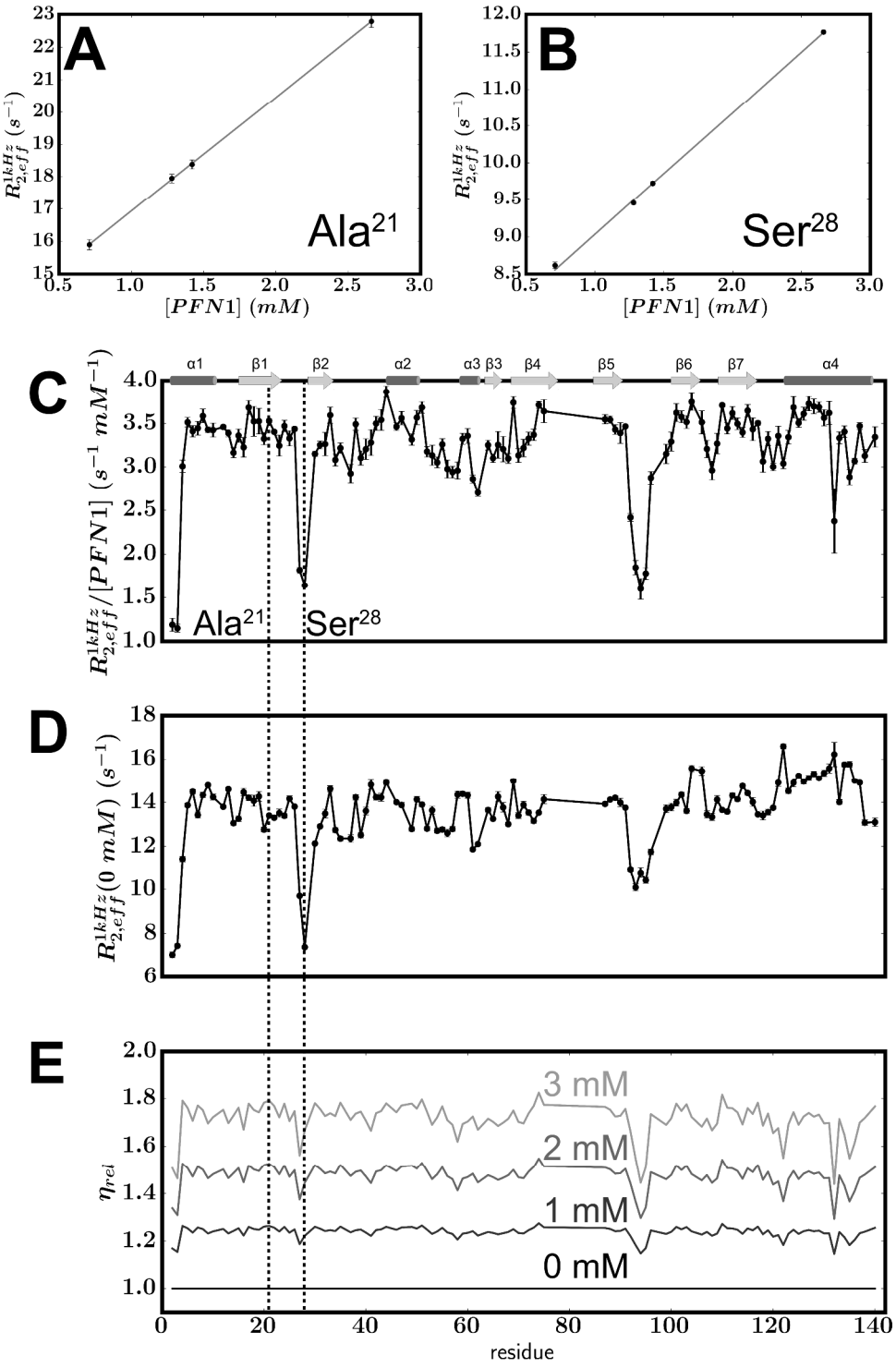

Figure S4. Linear increases in $R_{2,eff}^{1kHz}$ values with protein concentration, as shown for Ala^{21} (A) and Ser^{28} (B) of H134R PFN1 (that shows no evidence of chemical exchange). Note that the slope of $R_{2,eff}^{1kHz}$ *vs* [PFN1] is dependent on residue position; Ala^{21} is in strand β1, in

a rigid portion of the molecule, and its slope (3.5 s^{-1} mM^{-1}) and intercept (13.4 s^{-1}) are therefore larger than for Ser[28] that is located in a flexible loop (slope=1.6 s^{-1} mM^{-1}, intercept=7.4 s^{-1}). Slopes, intercepts and η_{rel}, as defined by Eq. [7] of the main text, $R_2^l([PFN1]) = R_2^l(0mM) \cdot \eta_{rel}$, are shown in panels C, D and E, respectively.

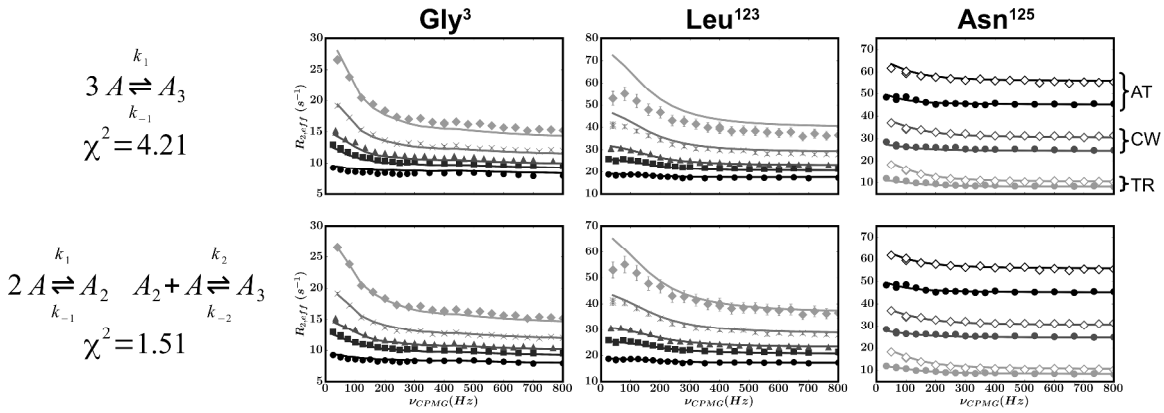

Figure S5. Fits of concentration dependent CPMG data for WT PFN1, as in Figure 5 of the main text, using additional models of oligomerization, as indicated. See legend to Figure 5 for additional details.

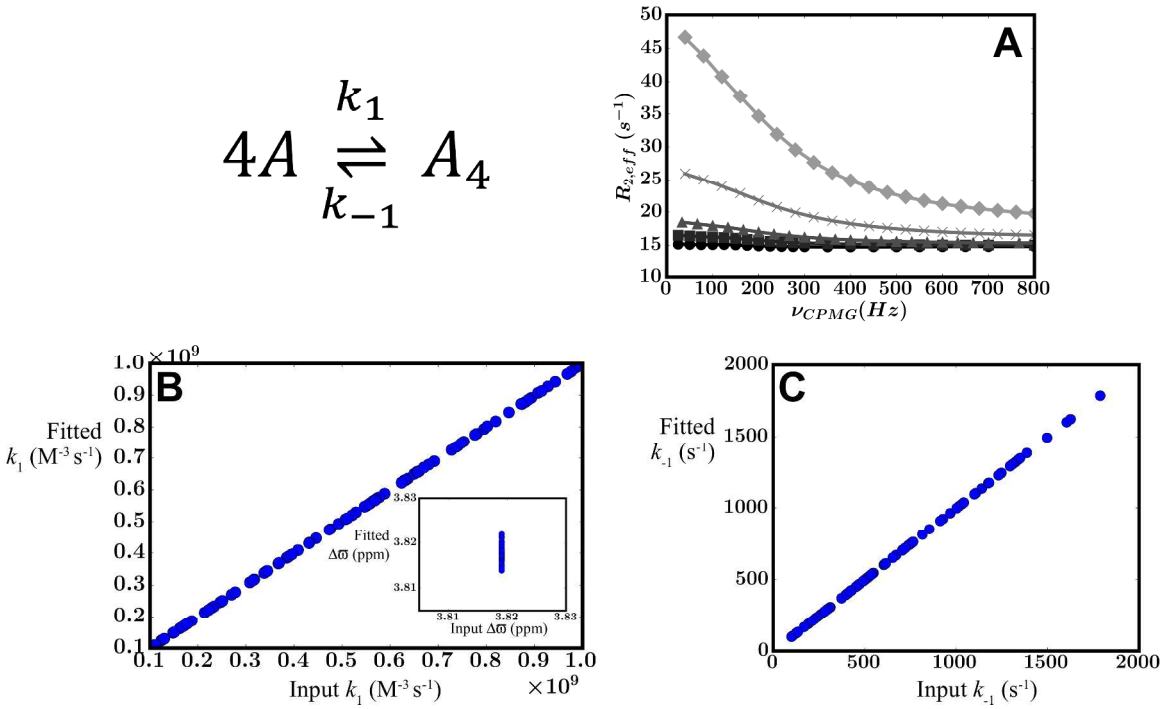

Figure S6. Two-state exchange data can be fit robustly: an example using the $4A \underset{k_{-1}}{\overset{k_1}{\rightleftharpoons}} A_4$ model. Data was simulated using the two-state monomer-tetramer exchange model with $\Delta\varpi$ values set to those obtained from fits of 6 experimental dispersion profiles to a pseudo two-state exchange model, $A \underset{k_{BA}}{\overset{k_{AB}}{\rightleftharpoons}} B$. Values for k_1 used to generate dispersion data were chosen randomly between 10^8 $M^{-3}s^{-1}$ – 10^9 $M^{-3}s^{-1}$ with k_{-1} obtained randomly from $0.5k_1$ /10^6– $2k_1$ /10^6, corresponding to p_{A_4} values ranging from 13% to 4.4%, respectively, for [PFN1]= 3mM. For each (k_1,k_{-1}) pair 6 dispersion profiles were generated (1 for each of the 6 experimental $\Delta\varpi$ values) at each of the 5 [PFN1] values used in the experiment. In all of the simulations the transverse relaxation rates of A and A_4 were set to 15 s^{-1} and 60 s^{-1}, respectively. Fits of the simulated profiles were initially performed using the pseudo two-state model and the obtained values then used as input for fitting with the $4A \underset{k_{-1}}{\overset{k_1}{\rightleftharpoons}} A_4$ model. (A) Fitted dispersion profiles for 1 residue (of the 6 used) along with correlation plots of fitted k_1 (B) and k_{-1} (C) values relative to those input, based on 100 simulations. It is noteworthy that although starting R_2 values were input as equal for monomer and tetramer in the final fits, the fitted rates were 15 s^{-1} and 60 s^{-1}, in agreement with those input. The inset to (B) shows the distribution of $\Delta\varpi$ values obtained for 1 residue (largest $\Delta\varpi$) from the 100 simulations.

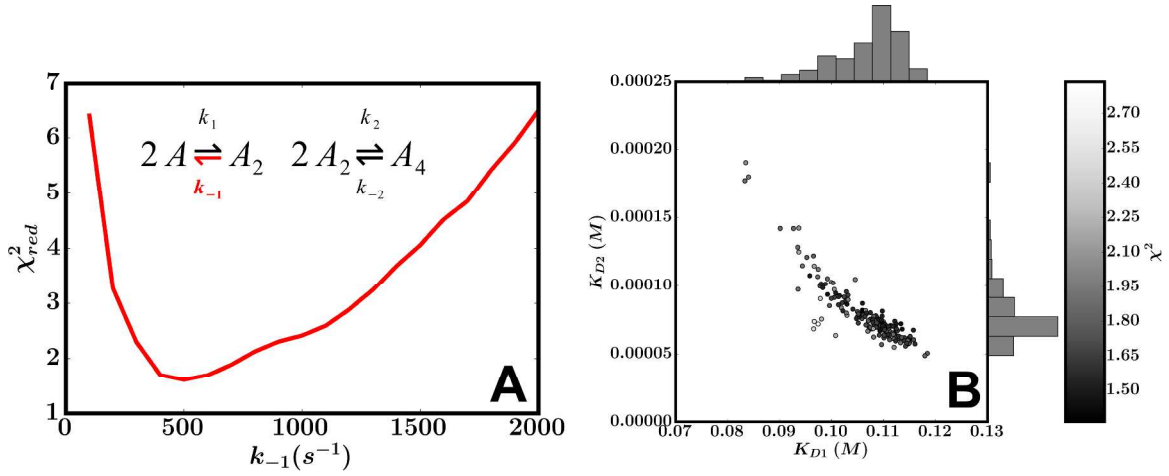

Figure S7. (A) χ^2_{red} surface for k_{-1} from a fit of the concentration dependent in-phase, TROSY and anti-TROSY data recorded on WT PFN1, 10°C, to the monomer-dimer-tetramer exchange model, as discussed in the text. (B) $K_{D2} = k_{-2}/k_2$ *vs* $K_{D1} = k_{-1}/k_1$, along with histograms of K_D values (top and right hand sides) obtained from a bootstrap analysis of CPMG data[3]. Values of reduced χ^2 obtained from each fit are indicated using the black-white color scale along the right side. The most probably K_{D1} and K_{D2} values, 10°C, are 110 mM and 60 μM, respectively.

Sample Derivation of A Chemical Exchange Model

Table 1 lists the exchange models that were used to fit the concentration dependent CPMG relaxation dispersion data. Palmer and coworkers have discussed exchange described by $nA \rightleftharpoons A_n$ [4] and in what follows we will consider the following scheme: $[2A \underset{k_{-1}}{\overset{k_1}{\rightleftharpoons}} A_2, 2A_2 \underset{k_{-2}}{\overset{k_2}{\rightleftharpoons}} A_4]$, in which a tetramer is formed via a set of sequential reactions. This model can explain the dispersion data reasonably well and in addition the tetrameric structure so formed is consistent with expectations based on X-ray studies of PFN2[1]. Focusing initially on concentrations and on the first reaction of the series $2A \underset{k_{-1}}{\overset{k_1}{\rightleftharpoons}} A_2$ we obtain

$$\begin{aligned} \frac{1}{2}\frac{d[A]}{dt} &= -k_1[A]^2 + k_{-1}[A_2] \\ \frac{d[A_2]}{dt} &= k_1[A]^2 - k_{-1}[A_2] \end{aligned} \qquad \text{[S1]}$$

while for $2A_2 \underset{k_{-2}}{\overset{k_2}{\rightleftharpoons}} A_4$

$$\begin{aligned} \frac{1}{2}\frac{d[A_2]}{dt} &= -k_2[A_2]^2 + k_{-2}[A_4] \\ \frac{d[A_4]}{dt} &= k_2[A_2]^2 - k_{-2}[A_4] \end{aligned} \qquad \text{[S2]}$$

Combining Eqs [S1] and [S2] it follows that,

$$\begin{aligned} \frac{d[A]}{dt} &= -2k_1[A]^2 + 2k_{-1}[A_2] \\ \frac{d[A_2]}{dt} &= -2k_2[A_2]^2 + 2k_{-2}[A_4] + k_1[A]^2 - k_{-1}[A_2] \\ \frac{d[A_4]}{dt} &= k_2[A_2]^2 - k_{-2}[A_4] \end{aligned} \qquad \text{[S3]}$$

Recalling that $M_A \propto [A]$, $M_{A_2} \propto 2[A_2]$, $M_{A_4} \propto 4[A_4]$ and linearizing Eq. [S3][5] we obtain

$$\begin{aligned}
\frac{dM_A}{dt} &= -2k_1[A]M_A + k_{-1}M_{A_2} \\
\frac{dM_{A_2}}{dt} &= -2k_2[A_2]M_{A_2} + k_{-2}M_{A_4} + 2k_1[A]M_A - k_{-1}M_{A_2} \\
\frac{dM_{A_4}}{dt} &= 2k_2[A_2]M_{A_2} - k_{-2}M_{A_4}
\end{aligned} \qquad \text{[S4]}$$

We can write the monomer-dimer-tetramer scheme $[2A \underset{k_{-1}}{\overset{k_1}{\rightleftharpoons}} A_2, 2A_2 \underset{k_{-2}}{\overset{k_2}{\rightleftharpoons}} A_4]$ as $[A \underset{k_{BA}}{\overset{k_{AB}}{\rightleftharpoons}} B, B \underset{k_{CB}}{\overset{k_{BC}}{\rightleftharpoons}} C]$ for which the following kinetic scheme holds,

$$\begin{aligned}
\frac{dM_A}{dt} &= -k_{AB}M_A + k_{BA}M_B \\
\frac{dM_B}{dt} &= k_{AB}M_A - k_{BA}M_B - k_{BC}M_B + k_{CB}M_C \\
\frac{dM_C}{dt} &= -k_{CB}M_C + k_{BC}M_B
\end{aligned} \qquad \text{[S5]}$$

Comparing Eqs [S4] and [S5] leads to the results of Table 1.

References

(1) Nodelman, I. M., Bowman, G. D., Lindberg, U., and Schutt, C. E. (1999) X-ray structure determination of human profilin II: A comparative structural analysis of human profilins. *J. Mol. Biol. 294*, 1271–1285.
(2) Metzler, W. J., Farmer, B. T., Constantine, K. L., Friedrichs, M. S., Lavoie, T., and Mueller, L. (1995) Refined solution structure of human profilin I. *Protein Sci. Publ. Protein Soc. 4*, 450–459.
(3) Choy, W.-Y., Zhou, Z., Bai, Y., and Kay, L. E. (2005) An 15N NMR spin relaxation dispersion study of the folding of a pair of engineered mutants of apocytochrome b562. *J. Am. Chem. Soc. 127*, 5066–5072.
(4) Palmer, A. G., Kroenke, C. D., and Loria, J. P. (2001) Nuclear magnetic resonance methods for quantifying microsecond-to-millisecond motions in biological macromolecules. *Methods Enzymol. 339*, 204–238.
(5) Sekhar, A., Bain, A. D., Rumfeldt, J. A. O., Meiering, E. M., and Kay, L. E. (2016) Evolution of magnetization due to asymmetric dimerization: theoretical considerations and application to aberrant oligomers formed by apoSOD1(2SH). *Phys. Chem. Chem. Phys. PCCP 18*, 5720–5728.